# Supporting Information

## Exploring Novel Ligands with Strong Electron Delocalization for High-performance Blue $CsPbBr_3$ Perovskite Nanoplatelets

*Zhuoqi Wen, Zhongjie Cui, Haiyang He, Dan Yang, Shiliang Mei*, Bobo Yang, Zhiyong Xiong, Shanliang Song, Rui Bao, Wanlu Zhang, Guichuan Xing, Fengxian Xie* and Ruiqian Guo**

## Experimental Section

*Chemicals*: Caesium carbonate ($Cs_2CO_3$, Aladdin, 99.99%), lead(II) bromide ($PbBr_2$, Macklin, 99.99%), oleic acid (OA, Aladdin, AR), oleylamine (OAm, Aladdin, C18:80-90%), 2-butynoic acid (BtA, Macklin, 98%), butyric acid (BA, Macklin, 99%), crotonic acid (CA, Macklin, ≥99.9%), phenylpropiolic acid (PA, Aladdin, ≥98.0%), 2-pentynoic acid (PtA, Aladdin, 97%), 1-octadecene (ODE, Aladdin, >90.0%), toluene (Tol, Sinopharm, ≥99.5%), acetone (Sinopharm, 99.5%), n-octane (Sinopharm, 98%) and methyl acetate (Macklin, 98%) were purchased without further purification.

*Preparation of precursors*: Cs-precursor was prepared by dissolving 0.4 mmol $Cs_2CO_3$ in 20 mL OA at 100 °C under continuous stirring. Pb-precursor was prepared by dissolving 0.3 mmol $PbBr_2$ in 10 mL Tol with 300 μL of OAm and OA at 100 °C. Different solution for post-treatment were prepared by mixing 1 mL OAm with 1 mL OA (OA/OAm), 3.15 mmol BtA (BtA/OAm), 3.15 mmol BA (BA/OAm), 3.15 mmol

CA (CA/OAm), 3.15 mmol PA (PA/OAm) and 3.15 mmol PtA (PtA/OAm) into 10 mL Tol.

*Preparation of perovskite NPLs (n=3)*: The perovskite NPLs were synthesized according to reported procedures with some modifications.[1] In a typical experiment, 450 μL Cs-precursor was injected into 3 mL Pb-precursor at room temperature with vigorous stirring. After 1 min, 5 mL acetone was added for initiating the formation of NPLs. Then, the turbid solution was centrifuged at 9000 rpm for 2 min and the obtained precipitate was redispersed in 2 mL Tol.

*The post-treatment of NPLs*: 400 μL of solution for post-treatment were dropped into the NPLs solution under vigorous stirring and further incubated in ambient atmosphere for 2 h. When investigating the influence of the concentration of ligands on NPLs, the precipitate was redispersed in 20 mL Tol and 10-80 μL of solution for post-treatment were added into 1 mL sample, respectively.

*Characterizations*: Absorption spectra were obtained through 759S Ultraviolet-visible spectrophotometer (Lengguang). PL spectra were recorded on F97XP spectrometer (Lengguang) with the excitation wavelength of 355 nm. Absolute PLQY values were measured using an integrating sphere within FluoroMax+ spectrometer (HORIBA) with the excitation wavelength of 355 nm. Transmission electron microscopy (TEM), high-resolution TEM (HRTEM) and selected area electron diffraction (SAED) images were obtained on JEM-2100F microscope (JEOL). Fourier transform infrared spectroscopy (FTIR) were obtained by Nicolet iS10 FTIR spectrophotometer (ThermoFisher). $^{1}$H-nuclear magnetic resonance ($^{1}$H-NMR) spectra were recorded on

AVANCE III HD 500MHz NMR spectrometer (Bruker). Time-resolved photoluminescence (TRPL) spectra were recorded on FS4 fluorescence spectrophotometer (Edinburgh). X-Ray Photoelectron Spectroscopy (XPS) were obtained on Axis Ultra DLD (Kratos). The XRD pattern was obtained using an X-ray diffractometer (Rigaku SmartLab 9kW) based on the NPLs films.

*Stability test of NPLs*: The solution of NPLs-OA/OAm, NPLs-BtA/OAm, NPLs-PA/OAm and NPLs-PtA/OAm were incubated at 80 ℃ or exposed to 365 nm UV light with the power density of 4 W $cm^{-2}$ with vigorous stirring and their PL spectra were recorded.

*DFT calculations*: First-principles calculations were carried out using DFT with generalized gradient approximation (GGA) of Perdew-Burke-Ernzerhof (PBE) implemented in the Vienna Ab-Initio Simulation Package (VASP).[2,3] The valence electronic states were expanded on the basis of plane waves with the core-valence interaction represented using the projector augmented plane wave (PAW) approach and a cutoff of 520 eV.[4] A Γ-centered k-mesh of 2 × 2 × 1 was used for the surface calculations. Convergence is achieved when the forces acting on ions become smaller than 0.02 eV $Å^{-1}$.

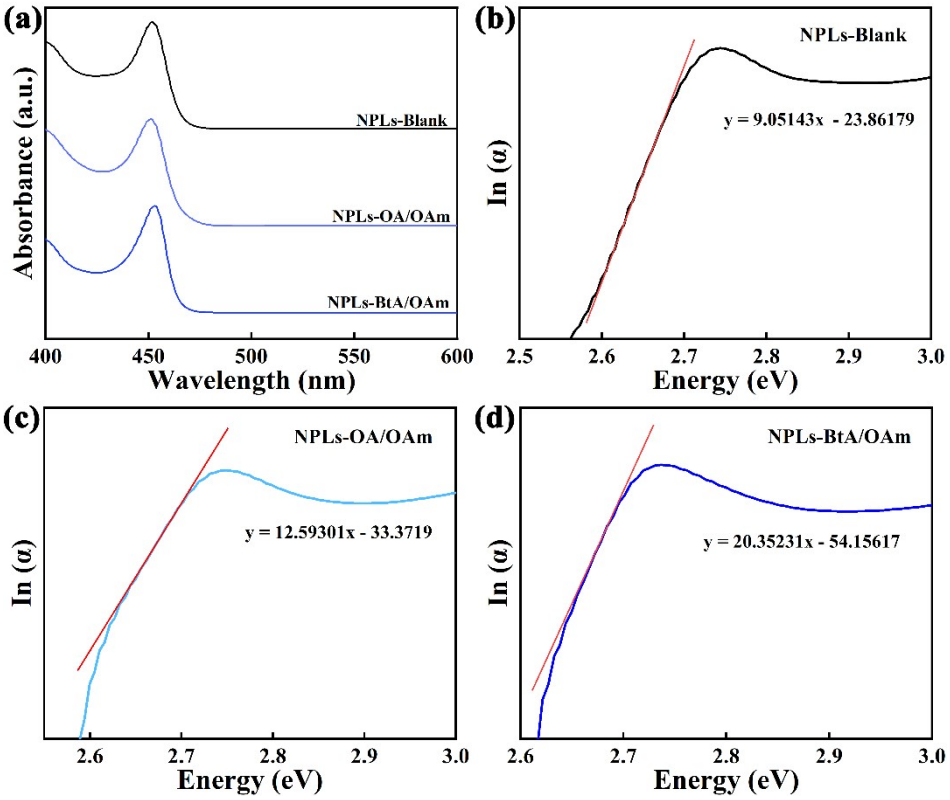


Figure S1. (a) Absorption spectra of NPLs-Blank, NPLs-OA/OAm and NPLs-BtA/OAm. Urbach energy diagrams of NPLs-Blank (b), PLs-OA/OAm (c) and NPLs-BtA/OAm (d).

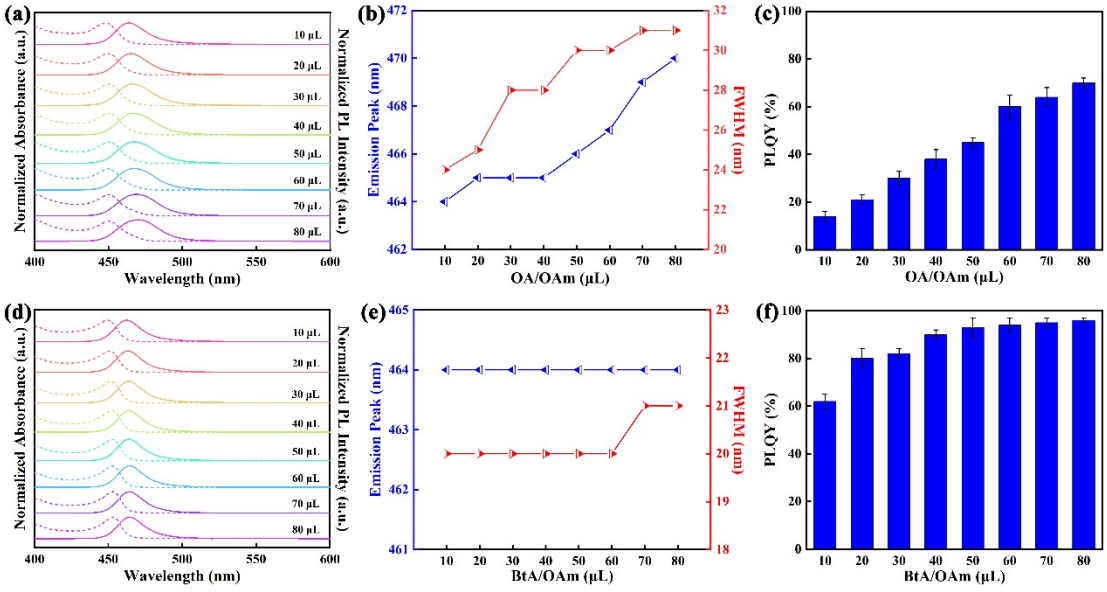


Figure S2. Normalized absorbance and PL spectra of NPLs-OA/OAm (a) and NPLs-BtA/OAm (d) with different ligand additions. The influence of ligand additions on emission peak and FWHM of NPLs-OA/OAm (b) and NPLs-BtA/OAm (e). The enhancement of ligand additions on PLQY of NPLs-OA/OAm (c) and NPLs-BtA/OAm (f).

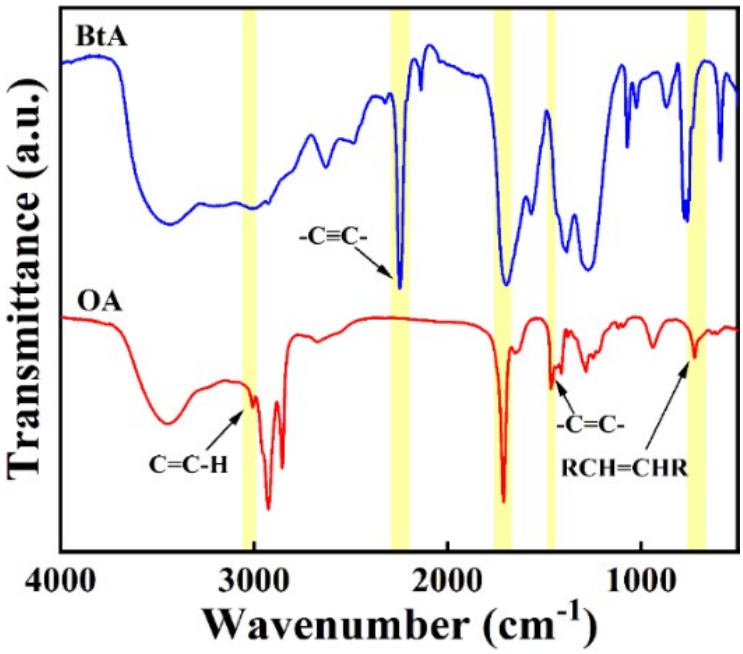


Figure S3. FTIR spectra of BtA and OA.

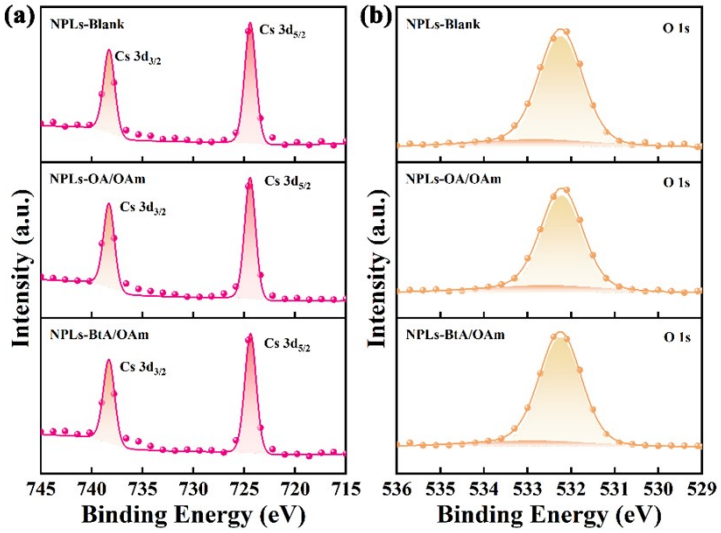


Figure S4. High-resolution XPS analyses of Cs 3d spectra (a) and O 1s spectra of original and post-treated NPLs.

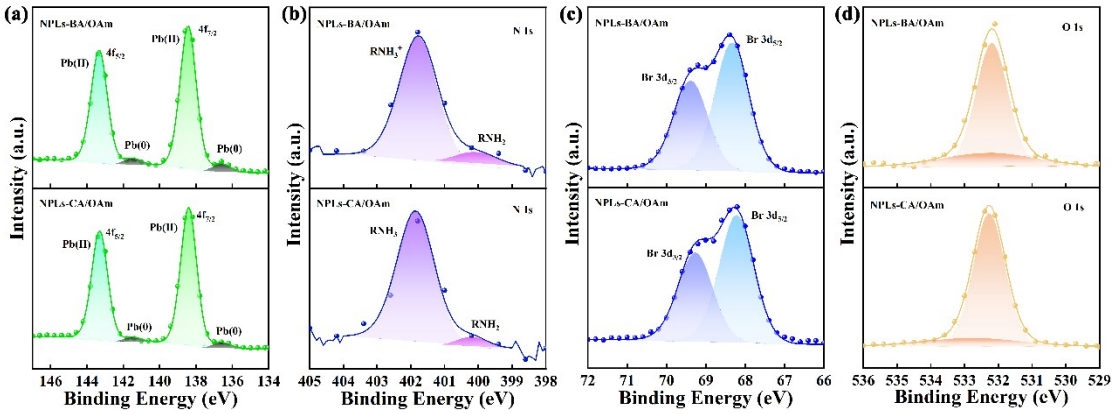


Figure S5. High-resolution XPS analyses of Pb 4f spectra (a), N 1s spectra (b) Br 3d spectra (c) and O 1s spectra (d) of NPLs-BA/OAm and NPLs-CA/OAm.

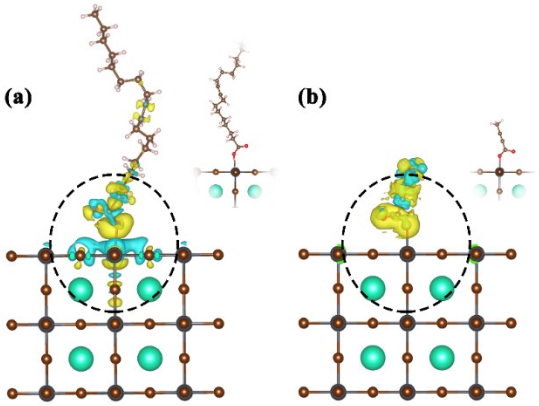


Figure S6. Deformation charge density of NPLs treated with OA (a) and BtA (b).

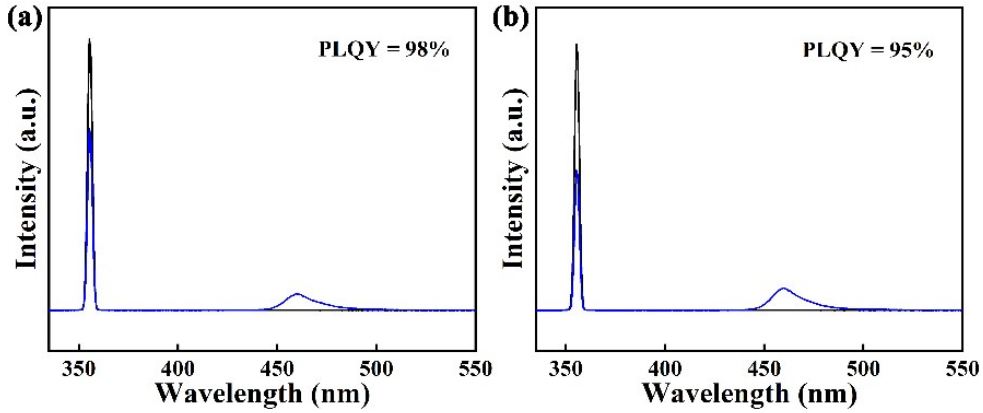


Figure S7. (a) PLQY measurement of NPLs-PA/OAm. (b) PLQY measurement of NPLs-PtA/OAm.

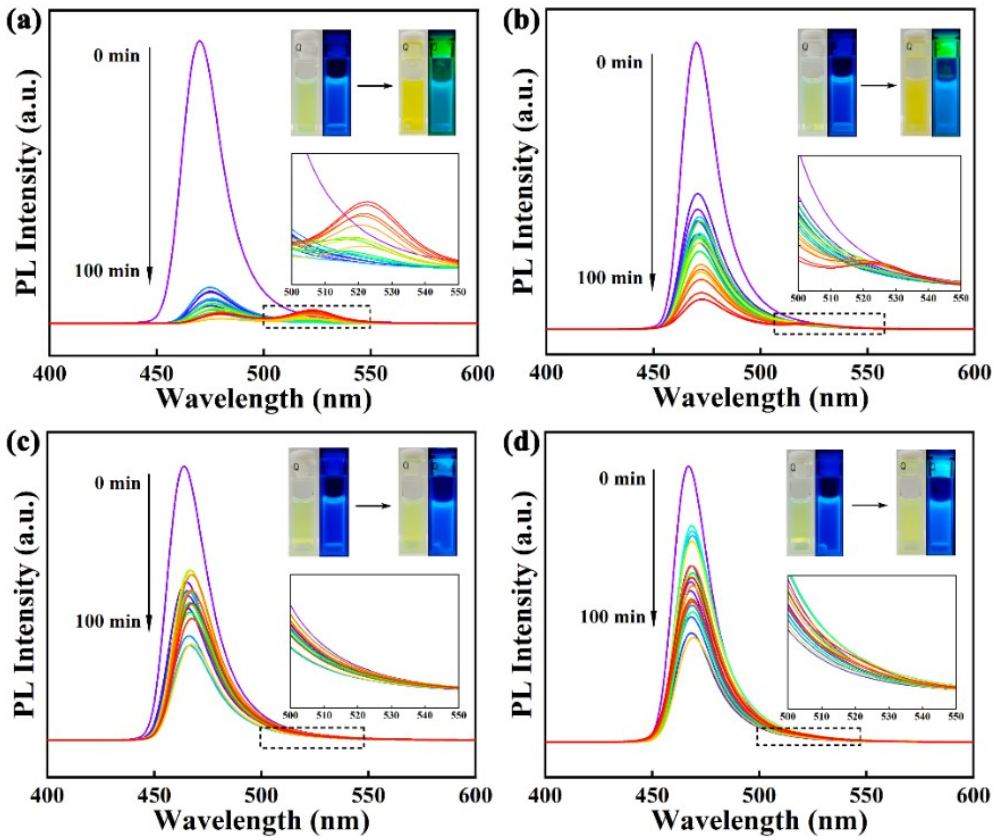


Figure S8. PL spectra of NPLs-OA/OAm (a), NPLs-BtA/OAm (b), NPLs-PA/OAm (c) and NPLs-PtA/OAm (d) under 80 °C for different times. The insets show photographs of NPLs before and after heating under ambient and UV light respectively.

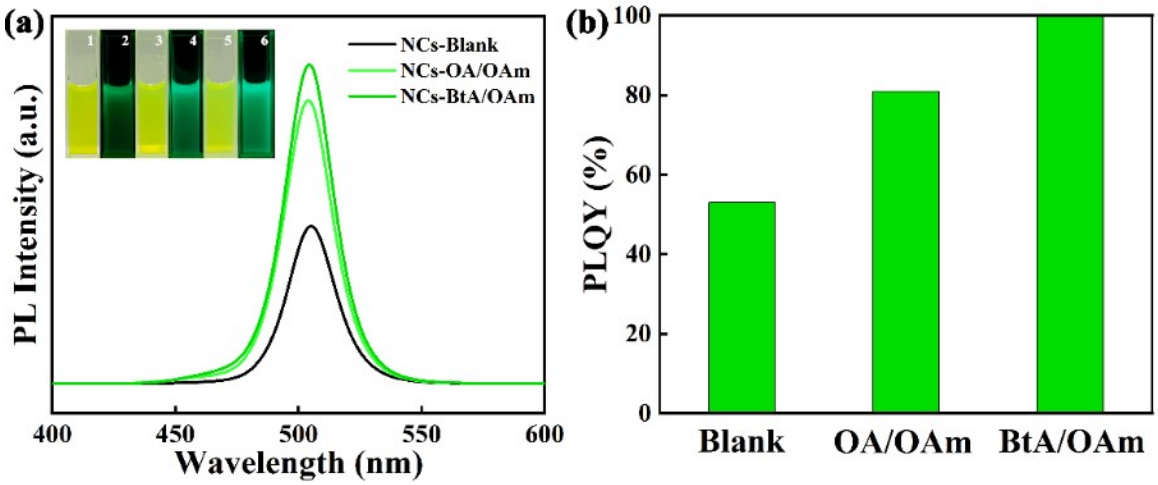


Figure S9. (a) PL spectra of original and post-treated NCs. The inset shows the photographs of NCs-Blank (1, 2), NCs-OA/OAm (3, 4) and NCs-BtA/OAm (5, 6) under ambient and UV light. (b) The enhancement of different ligands on PLQY of NCs.

Table S1. PL decay parameters of NPLs in Figure 1c.

| Sample | PLQY (%) | $\tau_1$ (ns) | $A_1$ | $\tau_2$ (ns) | $A_2$ | $\tau_{ave}$(ns) | $k_r$ ($ns^{-1}$) | $k_{nr}$ ($ns^{-1}$) |
|---|---|---|---|---|---|---|---|---|
| NPLs-Blank | 12±2 | 4.1 | 0.5 | 8.5 | 0.5 | 6.3 | 0.02 | 0.139 |
| NPLs-OA/OAm | 35±5 | 5.2 | 0.63 | 11.4 | 0.37 | 7.5 | 0.047 | 0.087 |
| NPLs-BtA/OAm | 87±5 | 6.1 | 0.53 | 15.5 | 0.47 | 10.5 | 0.083 | 0.012 |

Notes: $\tau_{ave} = \sum A_i\tau_i$; $k_r = PLQY/\tau_{ave}$; $k_{nr} = (1 - PLQY)/ \tau_{ave}$.

Table S2. Normalized element content of different NPLs measured by XPS.

| Sample | Cs | Pb | Br | N |
|---|---|---|---|---|
| NPLs-Blank | 0.75 | 1 | 2.83 | 0.87 |
| NPLs-OA/OAm | 0.63 | 1 | 2.94 | 1.13 |
| NPLs-BtA/OAm | 0.78 | 1 | 2.88 | 1.63 |
| NPLs-BA/OAm | 0.87 | 1 | 2.85 | 0.68 |
| NPLs-CA/OAm | 0.82 | 1 | 2.86 | 0.93 |

Table S3. Optical characteristics of blue-emitting $CsPbBr_3$ NPLs published to date.

| Sample | PL (nm) | PLQY (%) | Stability | Ref. |
|---|---|---|---|---|
| 1 | 460 | 14 (film) | No | [5] |
| 2 | 450 | 40 (film) | 30 min (heating at 50 °C) | [6] |
| 3 | 460 | ~70 | No | [7] |
| 4 | 462 | 96 | No | [8] |
| 5 | 457 | 85 | No | [9] |
| 6 | 460 | 98 | 1.5 year (stored in air) | [10] |
| 7 | 466 | 100 | 120 h (395 nm, 60 mW $cm^{-2}$) | [11] |
| 8 | 450 | 87 | 30 min (heating at 70 °C)<br>30 min (325 nm, 7 W $cm^{-2}$) | [12] |
| 9 | 460 | 60 | No | [13] |
| 10 | 462 | 10 | No | [14] |
| 11 | 460 | 98 | 120 min (400 nm, 110 mW $cm^{-2}$) | [15] |
| 12 | 465 | 70 | 68 h (stored in air) | [16] |
| 13 | 464 | 98 | 100 min (heating at 80 °C)<br>70 min (365 nm, 4 W $cm^{-2}$) | This work |

REFERENCE


1 S. Peng, Q. Wei, B. Wang, Z. Zhang, H. Yang, G. Pang, K. Wang, G. Xing, X. W. Sun and Z. Tang, *Angew. Chemie Int. Ed.*, 2020, **59**, 22156–22162.

2 J. P. Perdew, K. Burke and M. Ernzerhof, *Phys. Rev. Lett.*, 1996, **77**, 3865–3868.

3 G. Kresse and J. Furthmüller, *Phys. Rev. B*, 1996, **54**, 11169–11186.

4 P. E. Blöchl, *Phys. Rev. B*, 1994, **50**, 17953–17979.

5 R. L. Z. Hoye, M. L. Lai, M. Anaya, Y. Tong, K. Gałkowski, T. Doherty, W. Li, T. N. Huq, S. Mackowski, L. Polavarapu, J. Feldmann, J. L. Macmanus-Driscoll, R. H. Friend, A. S. Urban and S. D. Stranks, *ACS Energy Lett.*, 2019, **4**, 1181–1188.

6 J. Shamsi, D. Kubicki, D. Kubicki, M. Anaya, Y. Liu, K. Ji, K. Frohna, C. P. Grey, R. H. Friend, S. D. Stranks and S. D. Stranks, *ACS Energy Lett.*, 2020, **5**, 1900–1907.

7 H. Wang, F. Ye, J. Sun, Z. Wang, C. Zhang, J. Qian, X. Zhang, W. C. H. Choy, X. W. Sun, K. Wang and W. Zhao, *ACS Energy Lett.*, 2022, **7**, 1137–1145.

8 Y. Wu, C. Wei, X. Li, Y. Li, S. Qiu, W. Shen, B. Cai, Z. Sun, D. Yang, Z. Deng and H. Zeng, *ACS Energy Lett.*, 2018, **3**, 2030–2037.

9 W. Yin, M. Li, W. Dong, Z. Luo, Y. Li, J. Qian, J. Zhang, W. Zhang, Y. Zhang, S. V. Kershaw, X. Zhang, W. Zheng and A. L. Rogach, *ACS Energy Lett.*, 2021, 477–484.

10 S. Su, J. Tao, C. Sun, D. Xu, H. Zhang, T. Wei, Z. H. Zhang, Z. Wang, C. Fan and W. Bi, *Chem. Eng. J.*, , DOI:10.1016/j.cej.2021.129612.

11 H. Huang, W. Zhao, H. Yang, X. Zhang, J. Su, K. Hu, Z. Nie, Y. Li and J. Zhong, *J. Mater. Chem. C*, 2021, **9**, 5535–5543.

12 H. Lin, Q. Wei, K. W. Ng, J. Dong, J. Li, W. Liu, S. Yan, S. Chen, G. Xing, X. Tang, Z. Tang and S. Wang, *Small*, 2021, **17**, 2101359.

13 B. J. Bohn, Y. Tong, M. Gramlich, M. L. Lai, M. Döblinger, K. Wang, R. L. Z. Hoye, P. Müller-Buschbaum, S. D. Stranks, A. S. Urban, L. Polavarapu and J. Feldmann, *Nano Lett.*, 2018, **18**, 5231–5238.

14 Y. Bekenstein, B. A. Koscher, S. W. Eaton, P. Yang and A. P. Alivisatos, *J. Am. Chem. Soc.*, 2015, **137**, 16008–16011.

15 Q. Zeng, Y. Du, J. Jiang, Q. Yu and Y. Li, *J. Phys. Chem. Lett.*, 2021, **12**, 2668–2675.

16 C. Zhang, Q. Wan, B. Wang, W. Zheng, M. Liu, Q. Zhang, L. Kong and L. Li, *J. Phys. Chem. C*, 2019, **123**, 26161–26169.